

---

## Supporting Information

### **Ultra-Trace Detection of Methyl Parathion in Traditional Chinese Medicines Using a Gold Filament Enrichment Point Discharge Chemical Vapor Generation Atomic Emission Spectrometry**

Xin Yuan <sup>a\*</sup>, Yanping Wang <sup>a</sup>, Yuanjiao Yang <sup>a</sup>, Mei Zhang <sup>a</sup>, Ke Huang <sup>b\*</sup>

<sup>a</sup> State Key Laboratory of Southwestern Chinese Medicine Resources, School of Pharmacy, Chengdu University of Traditional Chinese Medicine, Chengdu, 611137, China

<sup>b</sup> College of Chemistry and Material Science, Sichuan Normal University, Chengdu, Sichuan, 610068, China

\*Corresponding author. E-mail: [yuanxin0330@163.com](mailto:yuanxin0330@163.com); [huangke@sicnu.edu.cn](mailto:huangke@sicnu.edu.cn)

---

## 1. Instrumentation

The microplasma was composed of a hollow cathode needle (1 mm i.d., 1.5 mm o.d., 15 mm length) and a stainless steel needle (1 mm diameter, 24 mm length), covering with the quartz tube (1 mm i.d., 3 mm o.d., 22 mm length). And the distance between the electrodes can be adjusted between 0.5 mm to 7 mm. Plasma power was provided from an AC power supply (Ray Man High Voltage ETC, MSP0310) with about 10 kV peak voltage. The working gas of this microplasma source is argon (Ar). Ar is introduced into the microplasma discharge region *via* a stainless steel hollow needle (carrier gas flow rate of 400 mL min<sup>-1</sup> controlled by a mass flow controller). When an AC voltage of 550 V or higher is applied between the two electrodes, a stable plasma can be generated in the gap between the tips of the two discharge needles.

In this work, Hg<sup>0</sup> vapor was enriched with a gold filament. A gold filament (30 μm diameter, 100 m length) was wrapped into a column and positioned in the central portion of a quartz tube (6 mm i.d., 8 mm o.d., 190 mm long), occupying a space of 32 mm. In order to prevent the gold filament from being blown out of the quartz tube by the carrier gas during the experiment, the quartz tube was flattened by high temperature to about 2 mm at a distance of about 70 mm from the outlet of the gas stream. The resistance wire (0.3 mm in diameter) was coiled around the outer surface of the quartz tube. Additionally, the heating temperature can be regulated by the transformer connected at both ends of the resistance wire.

---

## 2. The operation of PD-CVG-AES

The operation of the instrument consists of two steps: preconcentration and thermal desorption. In the preconcentration step,  $\text{SnCl}_2$  solutions were injected into the sample by using a syringe to generate  $\text{Hg}^0$  vapor. The generated  $\text{Hg}^0$  vapor flowed with argon through a vessel containing about 10 mL of concentrated  $\text{H}_2\text{SO}_4$  to remove traces of water. Subsequently, as the carrier gas (Ar) reached the gold filament, the  $\text{Hg}^0$  vapor was enriched through the gold filament to generate gold amalgam. In the thermal desorption step, the  $\text{Hg}^0$  vapor was stripped from the gold filament by heating and then transported to the PD microplasma. The radiation generated by the discharge was picked up by optical fiber (FDP600 SMA905-SMA905, 6.0 mm) and recorded by a CCD spectrometer (AvaSpec-ULS2048CL-2-EVO, Avantes, the Netherlands).

## 3. Reagents

All reagents used in this work are at least analytical grade. 1000 mg  $\text{L}^{-1}$  standard solutions of  $\text{Hg}^{2+}$ , methyl parathion, parathion, and carbendazim were purchased from Beijing North Weiye Measurement Technology Research Institute. Chlorpyrifos and imidacloprid were purchased from National Institute of Metrology.  $\text{SnCl}_2 \cdot \text{H}_2\text{O}$ , acetamiprid, butyrylcholinesterase, and Acetylthiocholine chloride were purchased from Maclin Biochemical Technology (Shanghai) Co., Ltd. Sucrose, ascorbic acid, NaCl,  $\text{FeCl}_3$ ,  $\text{ZnCl}_2$ ,  $\text{CuCl}_2$ , HCl,  $\text{MgSO}_4$ ,  $\text{C}_2\text{H}_3\text{NaO}_2$ , Acetonitrile, Methanol, sodium citrate and Acetic Acid were purchased from Kelong Reagent Factory (Chengdu, China). Phosphate buffered saline (PBS) was purchased from Sangon Biotech (Shanghai) Co., Ltd. Dispersion solid phase extraction purification tube was purchased

---

from Shimadzu (Shanghai) Experimental Equipment Co., LTD. *Panax ginseng*, *radix paeoniae alba*, *Angelica sinensis*, and *Lonicera japonica* were purchased from the Hehuachi professional market of Chinese Herbal Medicine in Chengdu. Ultrapure water (18.2 M $\Omega$  cm resistivity) was obtained from a UP water purification system.

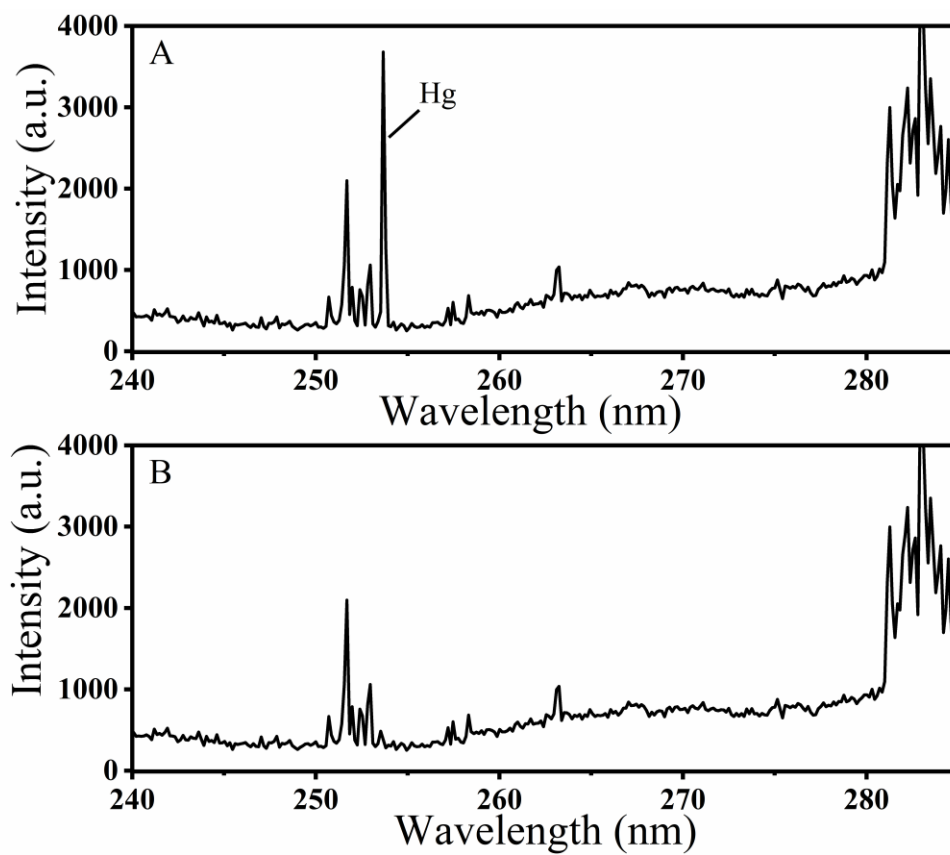


**Fig. S1.** Atomic emission lines generated with PD-CVG-AES at 253.67 nm. (A) 20 ng mL<sup>-1</sup> of Hg<sup>2+</sup>; (B) Blank.

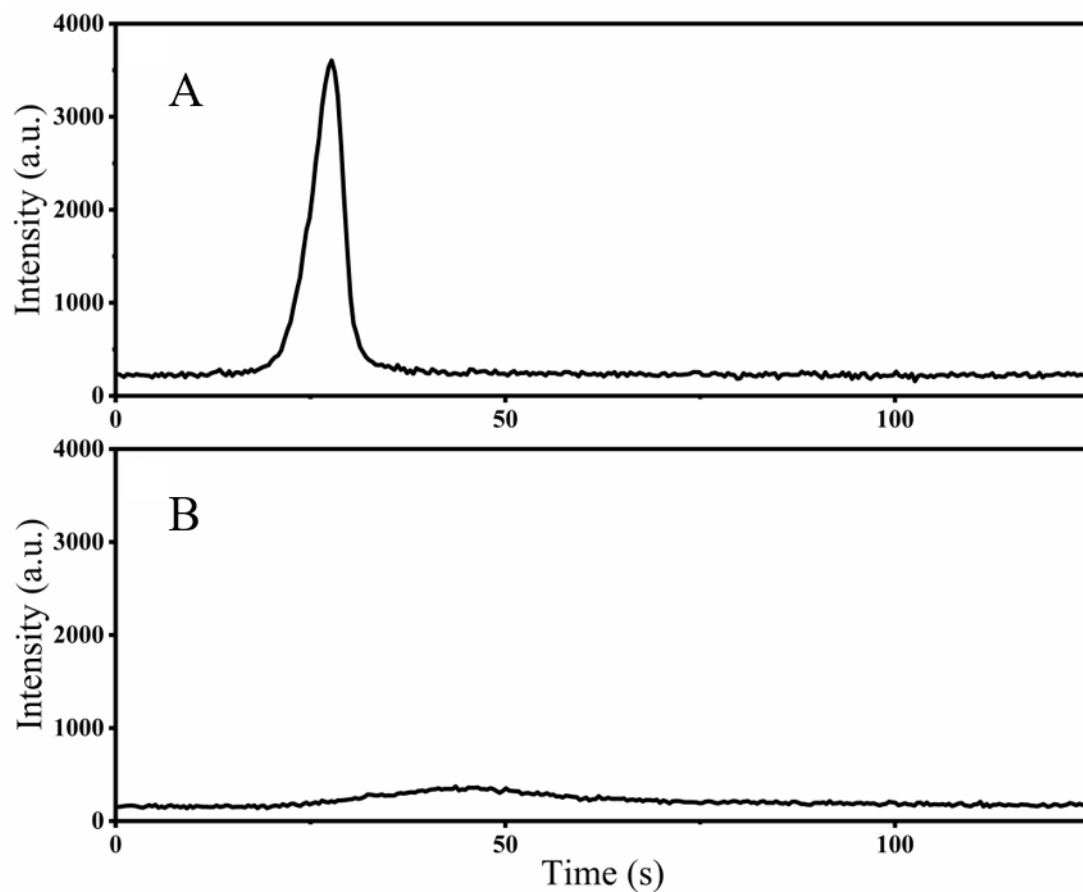


**Fig. S2.** Comparison of atomic emission lines generated with PD-CVG-AES at 253.67 nm. (A) With gold filament enrichment; (B) without gold filament enrichment. The concentration of  $\text{Hg}^{2+}$ :  $20 \text{ ng mL}^{-1}$ .

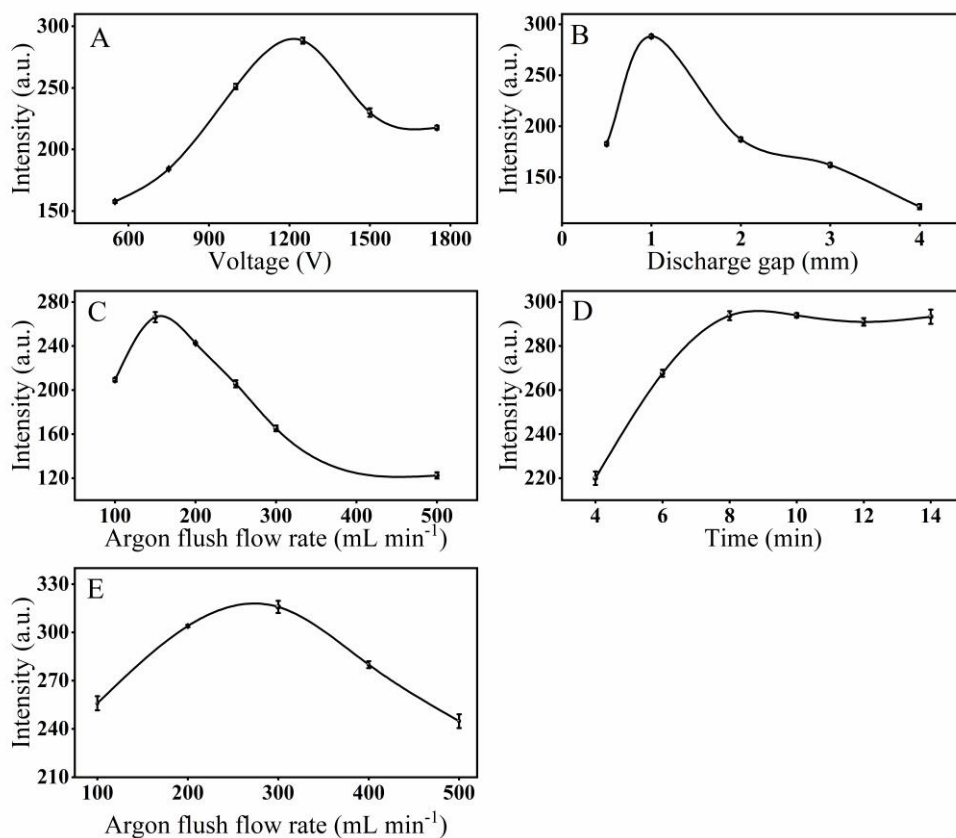


**Fig. S3.** Optimization of PD-CVG-AES Parameters involved several key factors: (A) voltage (V), (B) discharge gap (mm), (C) argon flush flow rate during the preconcentration step (mL min<sup>-1</sup>), (D) preconcentration time (min), and (E) argon flush flow rate during the thermal desorption step (mL min<sup>-1</sup>). Error bars represent the standard deviation from triplicate measurements.

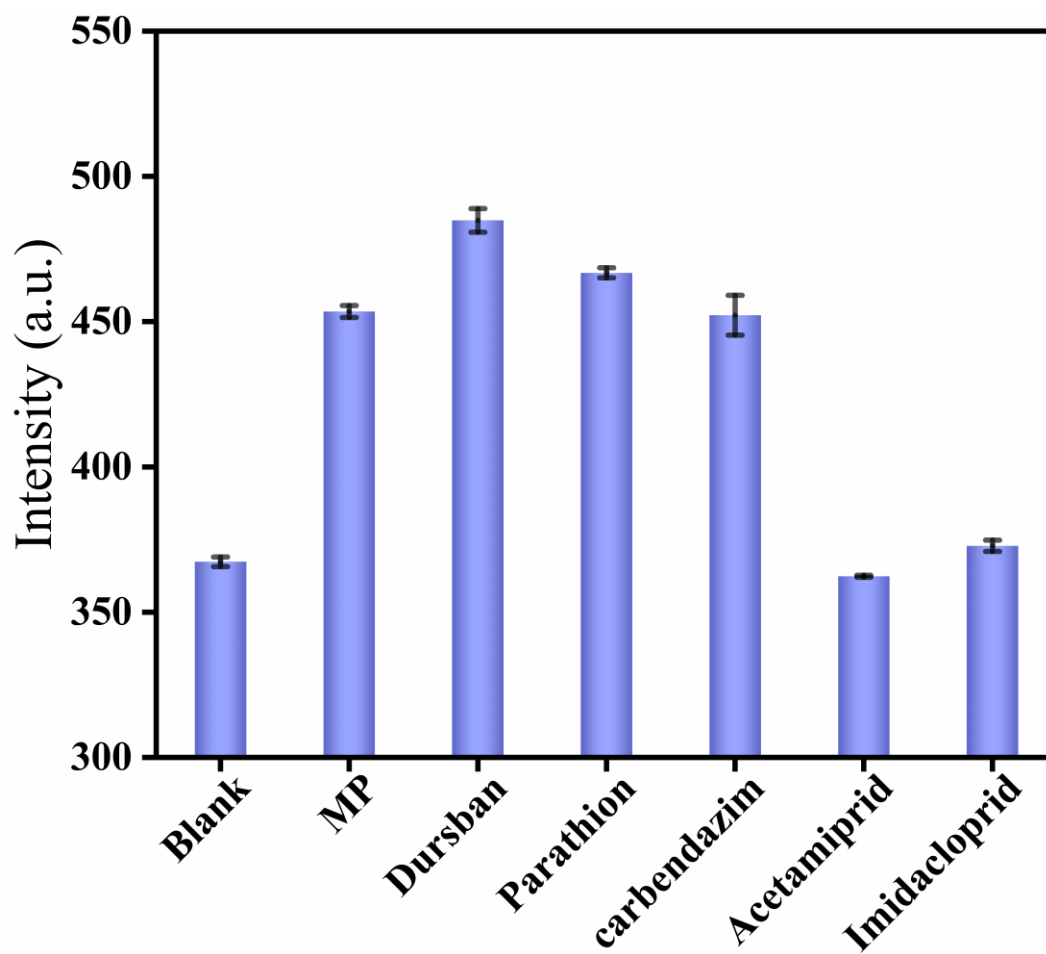


**Fig. S4.** Interference of various types of pesticides. Error bars originated from triplicate measurements.



---

**Table S1.** Operational parameters of PD-CVG-AES.

Parameter	Value
Reductant	SnCl <sub>2</sub> (1%, m/v)
Purging argon flow rate during preconcentration step (mL/min)	150
Preconcentration time (min)	8
Argon flow rate during thermal desorption step (mL/min)	250
Discharge current (mA)	2.5
Input voltage (V)	1250
Electrode distance (mm)	1
Integration time (ms)	200
Average	3

---

**Table S2.** Comparison of different methods for the determination of MP

Method	Samples	LOD	Reference
Fluorescence	apple and cucumber	3.3 ng mL <sup>-1</sup>	1
Fluorescence	water, apple, and carrot	32.4 ng mL <sup>-1</sup>	2
Fluorescence	apple, grape, cucumber, and tomato	0.14 μM	3
colorimetry	water, juice, vinegar, and fermented liquor	3 ng mL <sup>-1</sup>	4
SERS	apple	1.946 μg mL <sup>-1</sup>	5
SERS	juice	5 ng mL <sup>-1</sup>	6
Electrochemical	romaine and kiwifruit juice	0.034 μM	7
Electrochemical	Spinach, apple	0.01 μM	8
Electrochemical	ground water	1.21 ng mL <sup>-1</sup>	9
Electrochemical	grapes and tap water	8.9 ng mL <sup>-1</sup>	10
Biosensor	Chinese kale, Holy basil, Coriander, Morning glory, Asparagus, Durian, juice	0.1 μM	11
Headspace solid-phase microextraction	Rice	0.026 μg kg <sup>-1</sup>	12
GC-MS			
Magnetic solid phase extraction	Cabbage	13.9 ng g <sup>-1</sup>	13
GC-MS			
PD-CVG-AES	Panax ginseng, Angelica sinensis, radix paeoniae alba, and Lonicera japonica, Mentha	13 ng mL <sup>-1</sup>	This work

---

## References

1. J. Hu; H. Song; J. Zhou; R. Liu and Y. Lv, *Analytical Chemistry*, 2021, **93**, 14214-14222. <https://doi.org/10.1021/acs.analchem.1c03094>
2. Y. Li; M. Q. Wan; G. S. Yan; P. Qiu and X. L. Wang, *Journal of Pharmaceutical Analysis*, 2021, **11**, 183-190. <https://doi.org/10.1016/j.jpha.2020.04.007>
3. Y. Y. Yang; X. Tong; Y. X. Chen; R. R. Zhou; G. H. Cai; T. T. Wang; S. H. Zhang; S. Y. Shi and Y. Guo, *Food Chemistry*, 2023, **403**, 8. <https://doi.org/10.1016/j.foodchem.2022.134346>
4. X. Y. Bi; H. J. Jiang; X. L. Guo; M. Wang; Y. Niu; L. Y. Jia and X. Jing, *Rsc Advances*, 2022, **12**, 18127-18133. <https://doi.org/10.1039/d2ra02760g>
5. X. Y. Ma; J. Xie; Z. P. Wang and Y. Zhang, *Spectrochimica Acta Part a-Molecular and Biomolecular Spectroscopy*, 2022, **267**, 7. <https://doi.org/10.1016/j.saa.2021.120542>
6. A. N. Zhu; T. Xuan; Y. Zhai; Y. P. Wu; X. Y. Guo; Y. Ying; Y. Wen and H. F. Yang, *Sensors and Actuators B-Chemical*, 2021, **339**, 6. <https://doi.org/10.1016/j.snb.2021.129909>
7. H. Y. Zhao; H. N. Ma; X. G. Li; B. B. Liu; R. Q. Liu and S. Komarneni, *Applied Clay Science*, 2021, **200**, 10. <https://doi.org/10.1016/j.clay.2020.105907>
8. F. N. Zhao; J. W. He; X. J. Li; Y. P. Bai; Y. B. Ying and J. F. Ping, *Biosensors & Bioelectronics*, 2020, **170**, 8. <https://doi.org/10.1016/j.bios.2020.112636>
9. X. K. Tian; L. Liu; Y. Li; C. Yang; Z. X. Zhou; Y. L. Nie and Y. X. Wang, *Sensors and Actuators B-Chemical*, 2018, **256**, 135-142. <https://doi.org/10.1016/j.snb.2017.10.066>
10. R. X. Li; M. H. Shang; T. Zhe; M. Y. Li; F. E. Bai; Z. H. Xu; T. Bu; F. Li and L. Wang, *Journal of Hazardous Materials*, 2023, **447**, 10. <https://doi.org/10.1016/j.jhazmat.2023.130777>
11. W. Rapichai; S. Chaichalerm; J. Mearnchu and J. Wichitwechkarn, *Biotechnology Letters*, 2021, **43**, 933-944. <https://doi.org/10.1007/s10529-021-03078-1>
12. D. F. da Silva; F. E. Paiva Silva; F. G. S. Silva; G. S. Nunes and M. Badea, *Pest Management Science*, 2015, **71**, 1497-1502. <https://doi.org/10.1002/ps.3953>
13. L. Liu; M. Yang; M. He; T. Liu; F. Chen; Y. Li; X. Feng; Y. Zhang and F. Zhang, *Microchimica Acta*, 2020, **187**, 503. <https://doi.org/10.1007/s00604-020-04465-7>